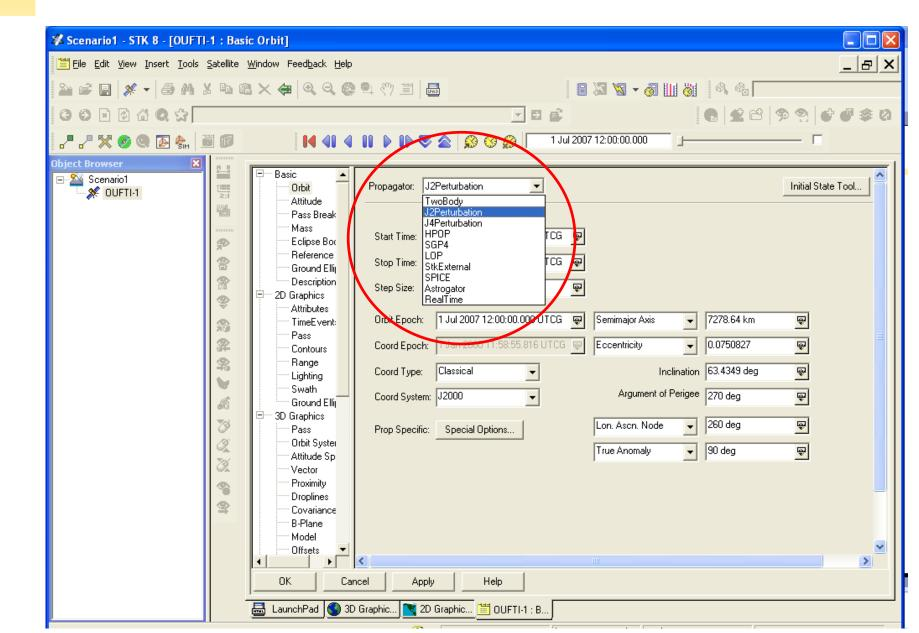


#### This lecture:

- 1. Effects of these perturbations on the orbital elements?
- 2. Computation of these effects?

### **STK: Different Propagators**



### **Why Different Propagators?**

#### Analytic propagation:

Better understanding of the perturbing forces.

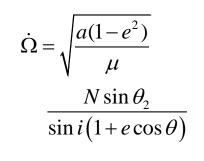
Useful for mission planning (fast answer): e.g., lifetime computation.

#### Numerical propagation:

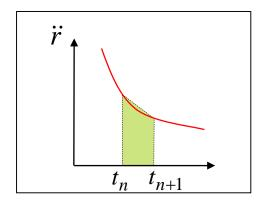
The high accuracy required today for satellite orbits can only be achieved by using numerical integration.

Incorporation of any arbitrary disturbing acceleration (versatile).

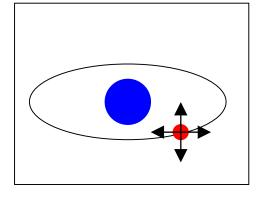
## 6. Non-Keplerian Motion



Analytic treatment



Numerical methods



ISS and geostationary satellites

### **Analytic Treatment: Definition**

Position and velocity at a requested time are computed directly from initial conditions in a single step.

Analytic propagators use a closed-form solution of the time-dependent motion of a satellite.

Mainly used for the two dominant perturbations, drag and earth oblateness.

### **Analytic Treatment: Pros and Cons**

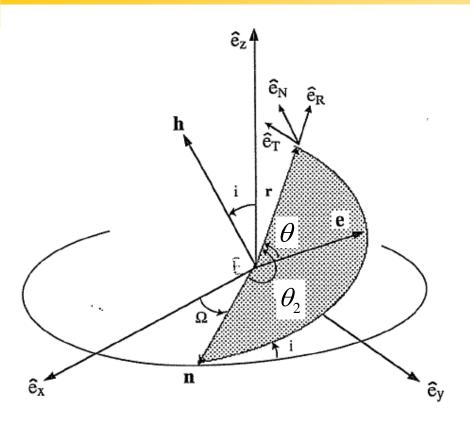
Useful for mission planning and analysis (fast and insight):

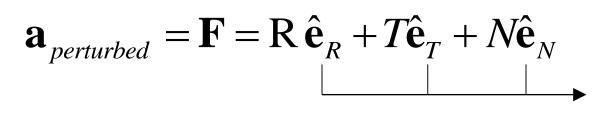
Though the numerical integration methods can generate more accurate ephemeris of a satellite with respect to a complex force model, the analytical solutions represent a manifold of solutions for a large domain of initial conditions and parameters.

But less accurate than numerical integration.

Be aware of the assumptions made!

### **Disturbing Acceleration (Specific Force)**





Rotating basis whose origin is fixed to the satellite

### **Variation of Parameters (VOP)**

Originally developed by Euler and improved by Lagrange (conservative) and Gauss (nonconservative).

It is called variation of parameters, because the orbital elements (i.e., the constant parameters in the two-body equations) are changing in the presence of perturbations. The energy and the angular momentum are no longer constant either.

The VOP equations are a system of first-order ODEs that describe the rates of change of the orbital elements.

$$\dot{a},\dot{i},\dot{e},\dot{\Omega},\dot{\omega},\dot{M}$$
?

## **Perturbation Equations (Gauss)**

$$\dot{\Omega} = \sqrt{\frac{a(1-e^2)}{\mu}} \frac{N\sin\theta_2}{\sin i(1+e\cos\theta)} \qquad \dot{a} = 2\sqrt{\frac{a^3}{\mu(1-e^2)}} \left[ \operatorname{Re}\sin\theta + T(1+e\cos\theta) \right]$$

$$\dot{i} = \sqrt{\frac{a(1-e^2)}{\mu}} \frac{N\cos\theta_2}{(1+e\cos\theta)} \qquad \dot{e} = \sqrt{\frac{a(1-e^2)}{\mu}} \left[ R\sin\theta + T(\cos\theta + \cos E) \right]$$

$$\dot{\omega} = -\dot{\Omega}\cos i + \frac{1}{e}\sqrt{\frac{a(1-e^2)}{\mu}} \left[ -R\cos\theta + \frac{T\sin\theta(2+e\cos\theta)}{1+e\cos\theta} \right]$$

$$M = nt - \chi, \text{ with } \dot{\chi} = \sqrt{\frac{a}{\mu}} \frac{(1-e^2)\left[ R(2e-\cos\theta-e\cos^2\theta) + T\sin\theta(2+e\cos\theta) \right]}{e(1+e\cos\theta)}$$

J.E. Prussing, B.A. Conway, Orbital Mechanics, Oxford University Press

## Let's demonstrate da/dt (energy variation)

$$\dot{a} = \frac{\mu}{2\varepsilon^2} \dot{\varepsilon} = \frac{2a^2}{\mu} \dot{\varepsilon}$$

$$\varepsilon = \frac{-\mu}{2a}$$

Energy of a satellite in elliptical orbit

$$\dot{\varepsilon} = \mathbf{F}\dot{\mathbf{r}} = \mathbf{F}\left(\dot{r}\hat{\mathbf{e}}_R + r\dot{\theta}\hat{\mathbf{e}}_T\right) = \dot{r}R + r\dot{\theta}T$$

Time rate-of-change of the work done by the disturbing force (power)

$$\dot{r} = \frac{ar}{d\theta}\dot{\theta}$$

$$\dot{r} = \frac{dr}{d\theta}\dot{\theta}$$
 &  $r = \frac{h^2}{\mu}\frac{1}{(1 + e\cos\theta)}$ 



$$\dot{r} = \frac{h^2}{\mu} \frac{e \sin \theta}{(1 + e \cos \theta)^2} \dot{\theta} = \frac{\mu r^2}{h^2} e \sin \theta \, \dot{\theta} = \frac{\mu e \sin \theta}{h}$$

$$\dot{\theta} = \frac{h^2}{r}$$

#### Let's demonstrate da/dt

$$\dot{a} = \frac{2a^2}{\mu} \left( \frac{\mu e \sin \theta}{h} R + \frac{h}{r} T \right) = \frac{2a^2}{h} \left( e \sin \theta R + \frac{h^2}{\mu r} T \right)$$
$$= \frac{2a^2}{h} \left( Re \sin \theta + T \left( 1 + e \cos \theta \right) \right)$$

$$h = \sqrt{\mu a(1 - e^2)}$$

$$\dot{a} = 2\sqrt{\frac{a^3}{\mu(1-e^2)}} \left( Re\sin\theta + T\left(1 + e\cos\theta\right) \right)$$

## Let's demonstrate de/dt (momentum variation)

$$\dot{\boldsymbol{h}} = \boldsymbol{r} \times \boldsymbol{F} = rT\hat{\boldsymbol{e}}_N - rN\hat{\boldsymbol{e}}_T$$
 Rotational motion 2<sup>nd</sup> law

The  $\hat{e}_T$  component is always normal to  $\mathbf{h}$ , so only the  $\hat{e}_N$  component changes the magnitude of  $\mathbf{h}$ 

$$\dot{h} = rT$$

$$h = \sqrt{\mu a (1 - e^2)} \quad \Box \qquad \dot{e} = \frac{1}{2} \left( 1 - \frac{h^2}{\mu a} \right)^{-1/2} \left[ \frac{-2h}{\mu a} \frac{dh}{dt} - \frac{h^2}{\mu a^2} \frac{da}{dt} \right]$$

$$\dot{e} = \frac{h}{\mu a e} r T + \frac{h^2}{2\mu a^2 e} \left( \frac{2e \sin \theta}{n\sqrt{1 - e^2}} R + \frac{2a\sqrt{1 - e^2}}{nr} T \right)$$

$$n = \sqrt{\mu/a^3}$$

## Let's demonstrate de/dt (momentum variation)

$$\dot{e} = \frac{h}{\mu a e} r T + \frac{h^2}{2\mu a^2 e} \left( \frac{2e \sin \theta}{n\sqrt{1 - e^2}} R + \frac{2a\sqrt{1 - e^2}}{nr} T \right)$$

$$n = \sqrt{\mu/a^3}$$

$$\dot{e} = \sqrt{\frac{a(1 - e^2)}{\mu}} \left( R \sin \theta + T(\cos \theta + \cos E) \right)$$

where E is the eccentric anomaly

## **Perturbation Equations (Gauss)**

$$\dot{\Omega} = \sqrt{\frac{a(1-e^2)}{\mu}} \frac{N\sin\theta_2}{\sin i(1+e\cos\theta)} \qquad \dot{a} = 2\sqrt{\frac{a^3}{\mu(1-e^2)}} \left[ \operatorname{Re}\sin\theta + T(1+e\cos\theta) \right]$$

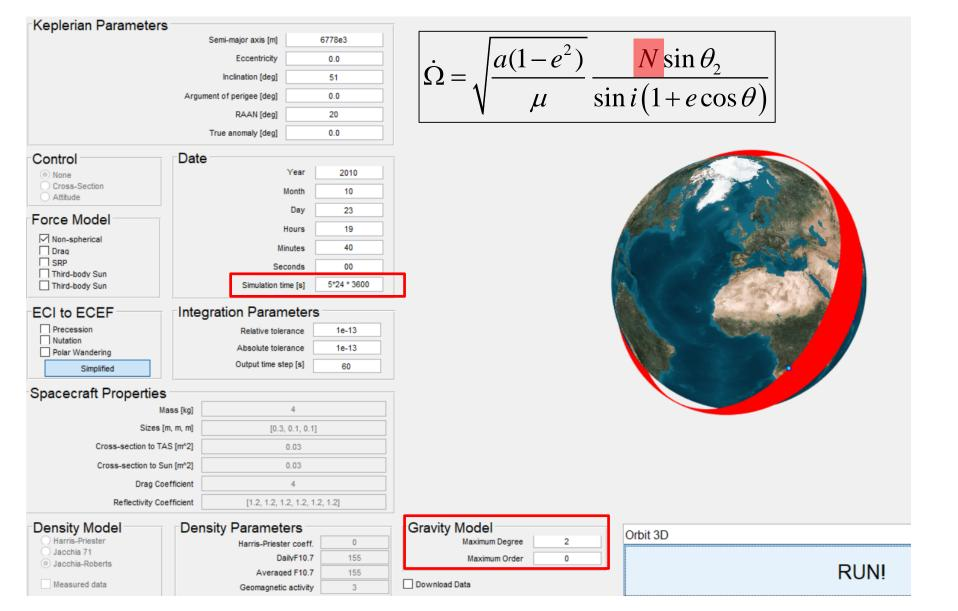
$$\dot{i} = \sqrt{\frac{a(1-e^2)}{\mu}} \frac{N\cos\theta_2}{(1+e\cos\theta)} \qquad \dot{e} = \sqrt{\frac{a(1-e^2)}{\mu}} \left[ R\sin\theta + T(\cos\theta + \cos E) \right]$$

$$\dot{\omega} = -\dot{\Omega}\cos i + \frac{1}{e}\sqrt{\frac{a(1-e^2)}{\mu}} \left[ -R\cos\theta + \frac{T\sin\theta(2+e\cos\theta)}{1+e\cos\theta} \right]$$

$$M = nt - \chi, \text{ with } \dot{\chi} = \sqrt{\frac{a}{\mu}} \frac{(1-e^2)\left[ R(2e-\cos\theta-e\cos^2\theta) + T\sin\theta(2+e\cos\theta) \right]}{e(1+e\cos\theta)}$$

J.E. Prussing, B.A. Conway, Orbital Mechanics, Oxford University Press

## Can We Predict the J2-Drift in Longitude?



# Disturbing Acceleration (Specific Force) for J2

$$U = \frac{\mu}{r} \left\{ 1 - J_2 \left( \frac{R_{\oplus}}{r} \right)^2 \frac{3\sin^2 \phi_{sat} - 1}{2} \right\}$$

$$\mathbf{F} = \nabla U \text{ with } \nabla = \hat{\mathbf{r}} \frac{\partial}{\partial r} + \frac{1}{r} \hat{\mathbf{\phi}} \frac{\partial}{\partial \phi} + \frac{1}{r \cos \phi} \hat{\lambda} \frac{\partial}{\partial \lambda}$$



$$\mathbf{F} = \frac{-3\mu J_2 R_{\oplus}^2}{r^4} \left[ \mathbf{e}_r \left( \frac{1 - 3\sin^2 i \sin^2 \theta}{2} \right) + \mathbf{e}_T \sin^2 i \sin \theta \cos \theta + \frac{\mathbf{e}_N \sin i \sin \theta \cos i}{2} \right]$$



$$\dot{\Omega} = \sqrt{\frac{a(1 - e^2)}{\mu}} \frac{N \sin \theta_2}{\sin i (1 + e \cos \theta)} \qquad \qquad \dot{\Omega}_{avg} = \frac{1}{T} \int_0^T \dot{\Omega} \, dt = -\left[ \frac{3}{2} \frac{\sqrt{\mu} J_2 R^2}{(1 - e^2)^2 a^{7/2}} \right] \cos i$$

### **Secular Effects: Node Line**

$$\dot{\Omega}_{avg} = \frac{1}{T} \int_0^T \dot{\Omega} \, dt = -\left[ \frac{3}{2} \frac{\sqrt{\mu} J_2 R^2}{(1 - e^2)^2 a^{7/2}} \right] \cos i$$

$$0 \le i \le 90^{\circ}, \dot{\Omega} < 0$$

⇒ For posigrade orbits, the node line drifts westward (regression of the nodes). And conversely.

$$i=90^{\circ}, \dot{\Omega}=0$$

 $\Rightarrow$  For polar orbits, the node line is stationary.

### **Analytical Prediction: the ISS case**

```
>> i=51/180*pi;a=(6378+400)*le3;muu=3.98600el4;J2=0.00108;R=6378e3;
>> omegadot=[-1.5*sqrt(muu)*J2*R^2/(a^3.5)*cos(i)]/pi*180*86400

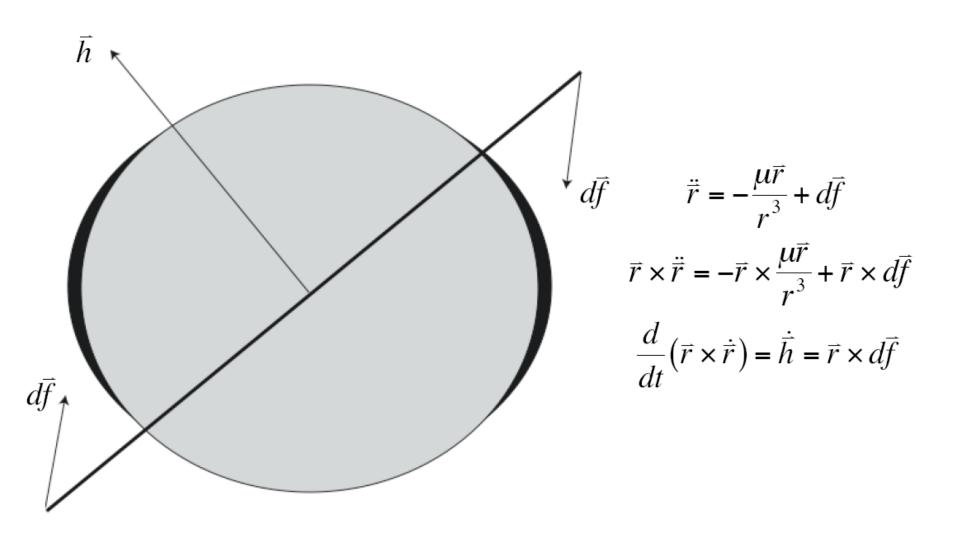
omegadot =
-5.0560
```

Analytical prediction: the drift in longitude for the ISS is 5 degrees per day

#### **Numerical Prediction: OK!**

```
Propagator_V1_16 ▶
%% Keplerian parameters
a0 = 6378e3 + 400e3; % [m] Semi-major axis
e0 = 0.00; % [] Eccentricity
i0 = deg2rad(51); % [rad] inclination
RAANO = deg2rad(0); % [rad] RAAN
omega0 = deg2rad(0); % [rad] Argument of periapsis
theta0 = deg2rad(0); % [rad] True anomaly
          360
          358
       356 (geg) NAAN (geg) 354
                                                                                X: 8.628e+04
                                                                                Y: 354.9
                                                                 360-354.9=5.1
          352
          350
                                      3
                                                               6
                                                                       7
                                                                               8
             0
                                                                                   \times 10^4
                                               Time (s)
```

### **Physical Interpretation of the Perturbation**

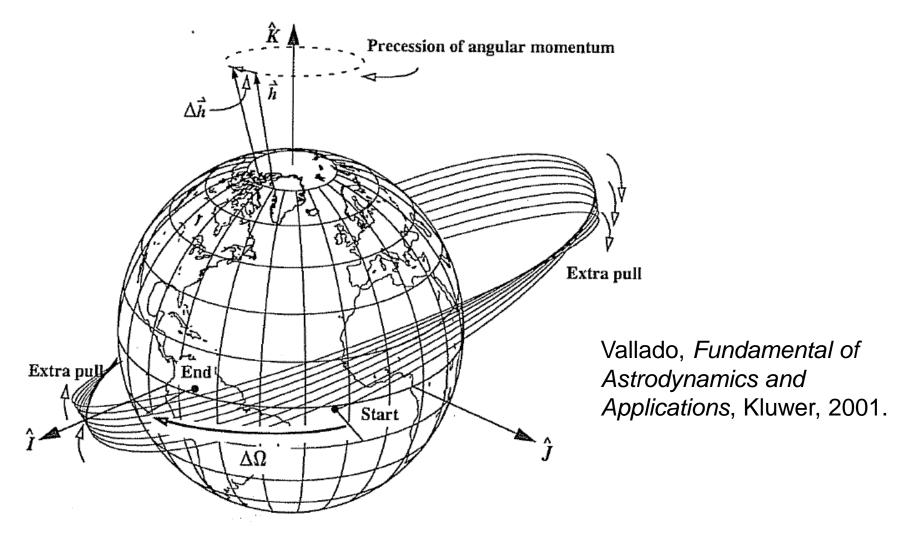


### **Physical Interpretation of the Perturbation**

The oblateness means that the force of gravity is no longer within the orbital plane: **non-planar motion will result**.

The equatorial bulge exerts a force that pulls the satellite back to the equatorial plane and thus tries to align the orbital plane with the equator.

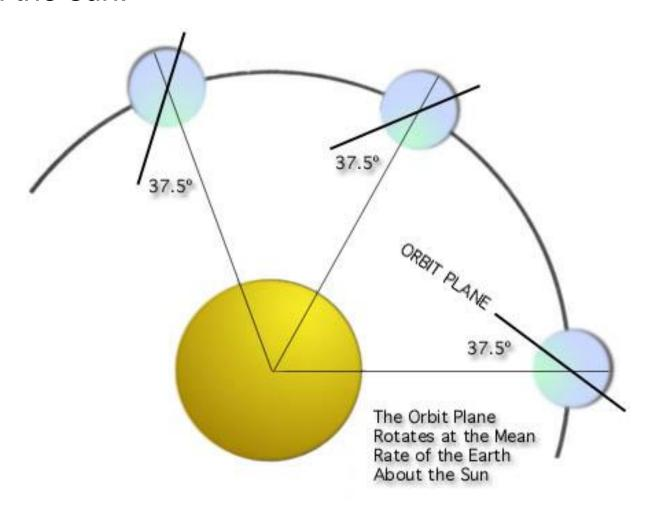
Due to its angular momentum, the orbit behaves like a spinning top and reacts with a precessional motion of the orbital plane (the orbital plane of the satellite to rotate in inertial space).



How Nodal Regression Works. The effect of a  $J_2$  perturbation that is 20 times the real value of  $J_2$  shows the precession of the longitude of ascending node. The perturbation manifests itself through a change in the angular-momentum vector, and the node regresses much like a precessing top. For this example, the correct interpretation is to say that the satellite's line of nodes experiences a rotation of  $50/8^{\circ}$  per revolution, or  $50^{\circ}$  per unit of time. The figure is also distorted because there is some apsidal rotation with an inclination not at the critical inclination (63.4°).

## Can We Exploit the Drift in Longitude?

The orbital plane makes a constant angle with the radial from the sun:



### **Yes! Sun-Synchronous Orbits**

The orbital plane must rotate in inertial space with the angular velocity of the Earth in its orbit around the Sun:

360° per 365.26 days or 0.9856° per day

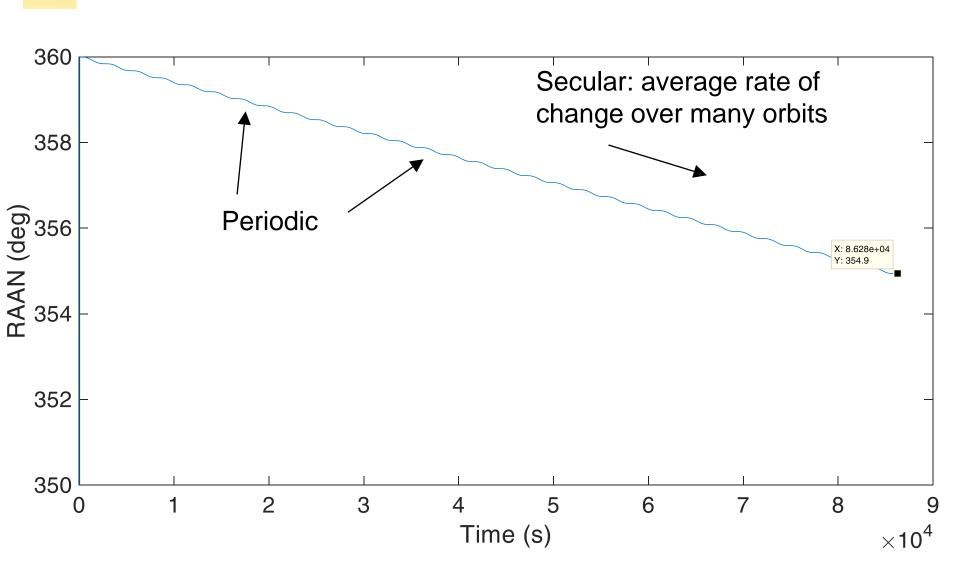
The satellite sees any given swath of the planet under nearly the same condition of daylight or darkness day after day.

### **Example of SPOT-5 Satellite**



```
>> i=98.7/180*pi;a=(6378+820)*le3;muu=3.98600el4;J2=0.00108;R=6378e3;
>> omegadot=[-1.5*sqrt(muu)*J2*R^2/(a^3.5)*cos(i)]/pi*180*86400
omegadot =
0.9846
```

### **Effect of Perturbations on Orbital Elements**



## **Secular Effects: Apse Line**

$$\dot{\omega}_{avg} = \frac{1}{T} \int_0^T \dot{\omega} \, dt = \left[ \frac{3}{4} \frac{\sqrt{\mu} J_2 R^2}{(1 - e^2)^2 a^{7/2}} \right] (4 - 5\sin^2 i)$$

$$0^{\circ} \le i \le 63.4^{\circ} \text{ or } 116.6^{\circ} \le i \le 180^{\circ}, \dot{\omega} > 0$$

⇒ The perigee advances in the direction of the motion of the satellite. And conversely.

$$i = 63.4^{\circ} \text{ or } i = 116.6^{\circ}, \dot{\omega} = 0$$

 $\Rightarrow$  The apse line does not move.

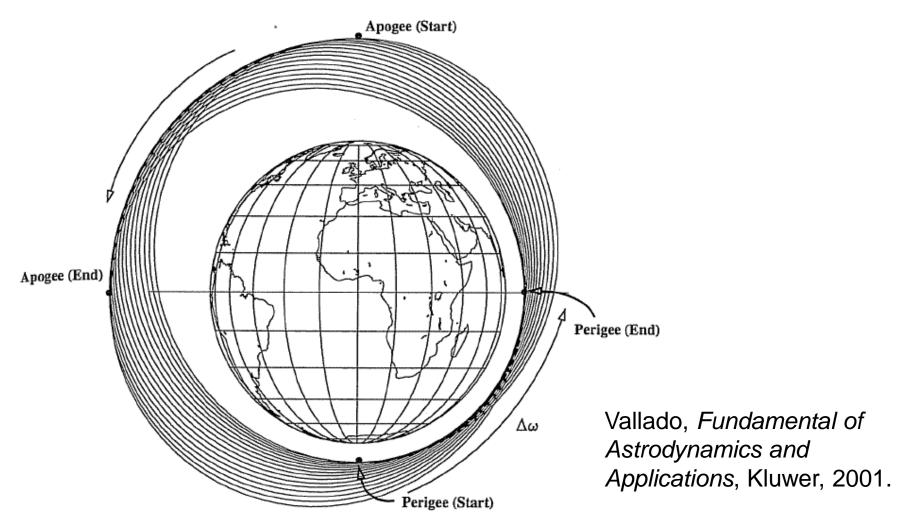


Figure 9-5. How Apsidal Rotation Works. We can see the effect of apsidal rotation after the  $J_2$  perturbation effect increases by a factor of 40 for a polar orbit (to eliminate the nodal regression). Notice how perigee (and apogee) locations change dramatically in a few revolutions.

## Can We Exploit the Drift of the Perigee?

A geostationary satellite cannot view effectively the far northern latitudes into which Russian territory extends (+ costly plane change maneuver for the launch vehicle!)

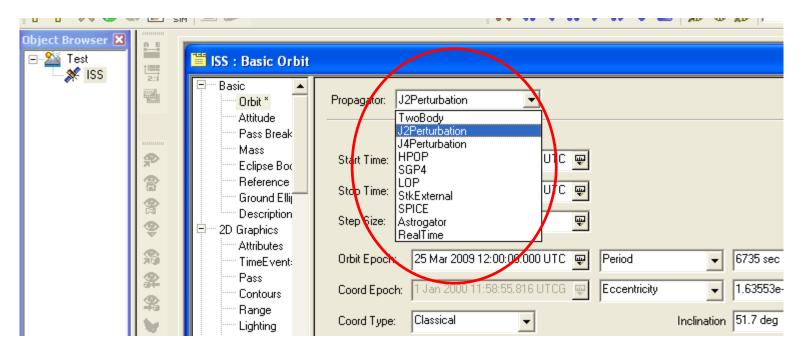
Molniya telecommunications satellites are launched from Plesetsk (62.8°N) into 63° inclination orbits having a period of 12 hours.

$$T_{ellip} = 2\pi \sqrt{\frac{a^3}{\mu}}$$
  $\rightarrow$  the apse line is 53000 km long.

### **Analytic Propagators in STK: 2-body, J2**

2-body: constant orbital elements.

J2: accounts for secular variations in the orbit elements due to Earth oblateness; periodic variations are neglected.



### J2 Propagator: Underlying Equations

$$\overline{n} = n \left[ 1 + \frac{3}{2} J_2 \frac{R_e^2}{p^2} \sqrt{1 - e^2} \left( 1 - \frac{3}{2} \sin^2 i \right) \right] \qquad \omega = \omega_0 + \left( \frac{3}{2} J_2 \frac{R_e^2}{p^2} \left[ 2 - \frac{5}{2} \sin^2 i \right] \right) \overline{n} (t - t_0)$$

$$\Omega = \Omega_0 - \left( \frac{3}{2} J_2 \frac{R_e^2}{p^2} \cos i \right) \overline{n} (t - t_0)$$

$$M = M_0 + \overline{n} (t - t_0)$$

$$\frac{259,50}{259,00}$$

$$\frac{259,50}{255,50}$$

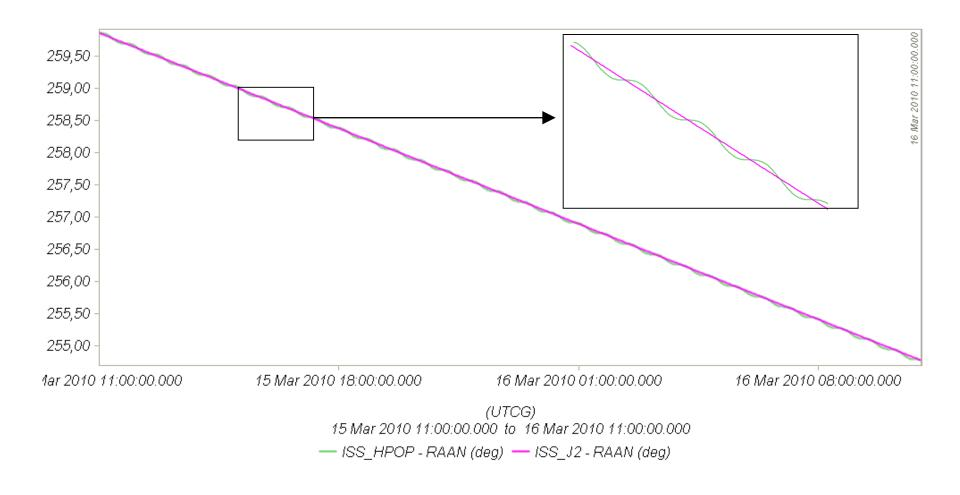
$$\frac{256,50}{255,00}$$

$$\frac{256,50}{255,00}$$

$$\frac{259,50}{255,00}$$

$$\frac{259,50}$$

### **HPOP and J2 Propagators Applied to ISS**



## Effects of Atmospheric Drag: Semi-Major Axis

$$\dot{a} = \frac{\mu}{2\varepsilon^2} \dot{\varepsilon} = \frac{2a^2}{\mu} \dot{\varepsilon}$$

Because drag causes the dissipation of mechanical energy from the system, the semimajor axis contracts.

Drag paradox: the effect of atmospheric drag is to increase the satellite speed and kinetic energy!

## Effects of Atmospheric Drag: Semi-Major Axis

$$N = R = 0, \quad T = -\frac{1}{2}C_{D}\frac{A}{m}\rho v_{r}^{2} = -\frac{1}{2}C_{D}\frac{A}{m}\rho\frac{\mu}{a}$$

$$\dot{a} = 2\sqrt{\frac{a^{3}}{\mu(1-e^{2})}}\left[\operatorname{Re}\sin\theta + T(1+e\cos\theta)\right]$$

$$Circular \text{ orbit}$$

$$\dot{a} = -\sqrt{a\mu\rho}C_{D}\frac{A}{m} < 0$$

$$ho$$
 is assumed constant

$$\sqrt{a_f} - \sqrt{a_i} = \frac{-\sqrt{\mu}\rho C_D A}{2m} \left(t_f - t_i\right)$$

## **Effects of Atmospheric Drag: Orbit Plane**

$$\dot{\Omega} = \sqrt{\frac{a(1-e^2)}{\mu}} \frac{N\sin\theta_2}{\sin i (1 + e\cos\theta)}$$

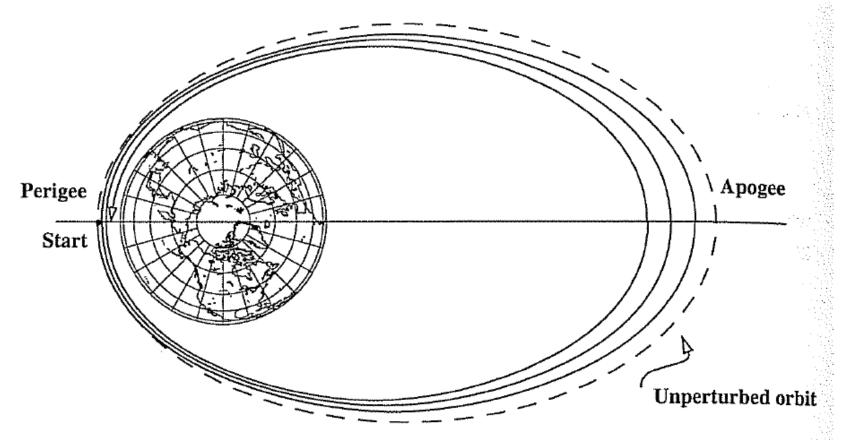
$$\dot{i} = \sqrt{\frac{a(1-e^2)}{\mu}} \frac{N\cos\theta_2}{(1+e\cos\theta)}$$



The orientation of the orbit plane is not changed by drag.

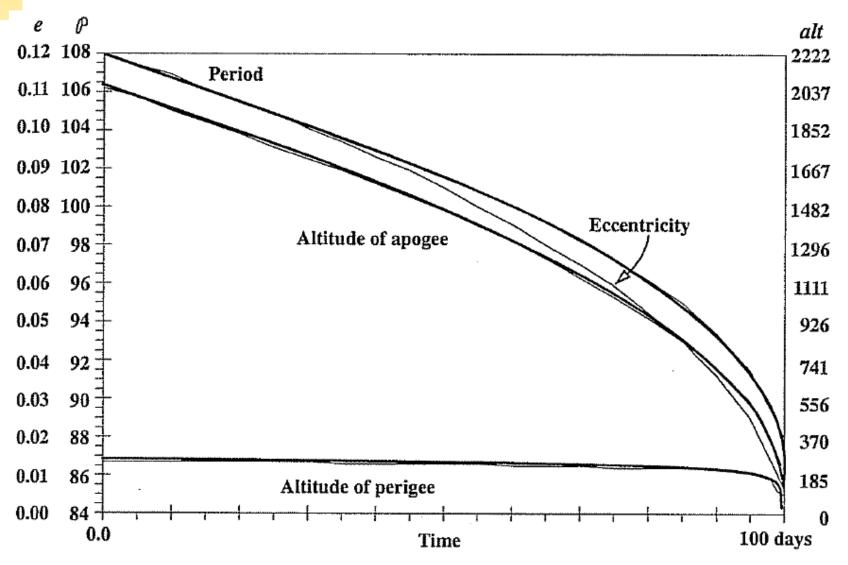
#### Effects of Atmospheric Drag: Apogee, Perigee

Apogee height changes drastically, perigee height remains relatively constant.



Vallado, Fundamental of Astrodynamics and Applications, Kluwer, 2001.

#### **Effects of Atmospheric Drag: Eccentricity**



Vallado, Fundamental of Astrodynamics and Applications, Kluwer, 2001.

#### Early Reentry of Skylab (1979)

Increased solar activity, which increased drag on Skylab, led to an early reentry.

Earth reentry footprint could not be accurately predicted (due to tumbling and other parameters).

Debris was found around Esperance (31–34°S, 122– 126°E). The Shire of Esperance fined the United States \$400 for littering, a fine which, to this day, remains unpaid.



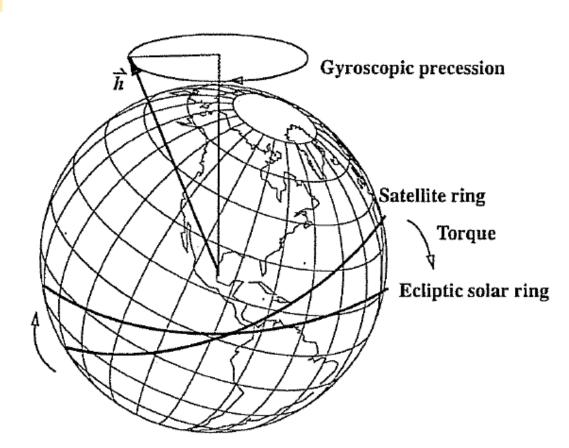
#### **Effects of Third-Body Perturbations**

The only secular perturbations are in the node and in the perigee.

For near-Earth orbits, the dominance of the oblateness dictates that the orbital plane regresses about the polar axis. For higher orbits, the regression will be about some mean pole lying between the Earth's pole and the ecliptic pole.

Many geosynchronous satellites launched 30 years ago now have inclinations of up to  $\pm 15^{\circ} \Rightarrow$  collision avoidance as the satellites drift back through the GEO belt.

#### **Effects of Third-Body Perturbations**



The Sun's attraction tends to turn the satellite ring into the ecliptic. The orbit precesses about the pole of the ecliptic.

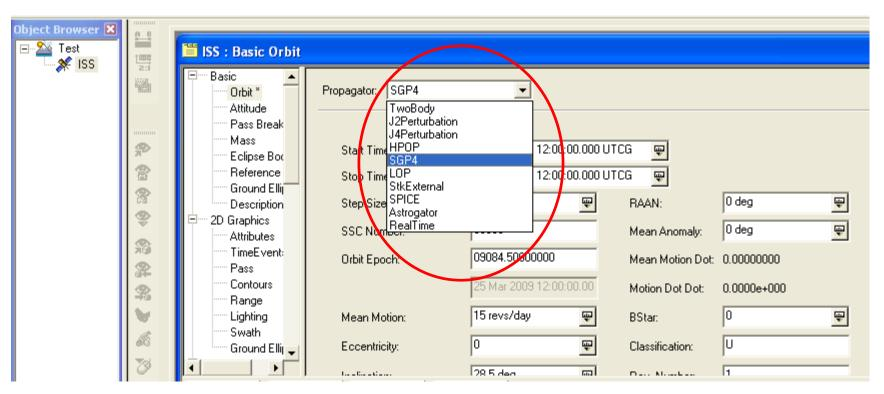
**Third-Body Interactions.** Imagine that the entire mass of a third body (the Sun, for instance) occupies a band about the planet. The resulting torque causes the satellite's orbit to precess like a gyroscope.

Vallado, Fundamental of Astrodynamics and Applications, Kluwer, 2001.

#### **STK: Analytic Propagator (SGP4)**

The J2 propagator does not include drag.

SGP4, which stands for Simplified General Perturbations Satellite Orbit Model 4, is a NASA/NORAD algorithm.



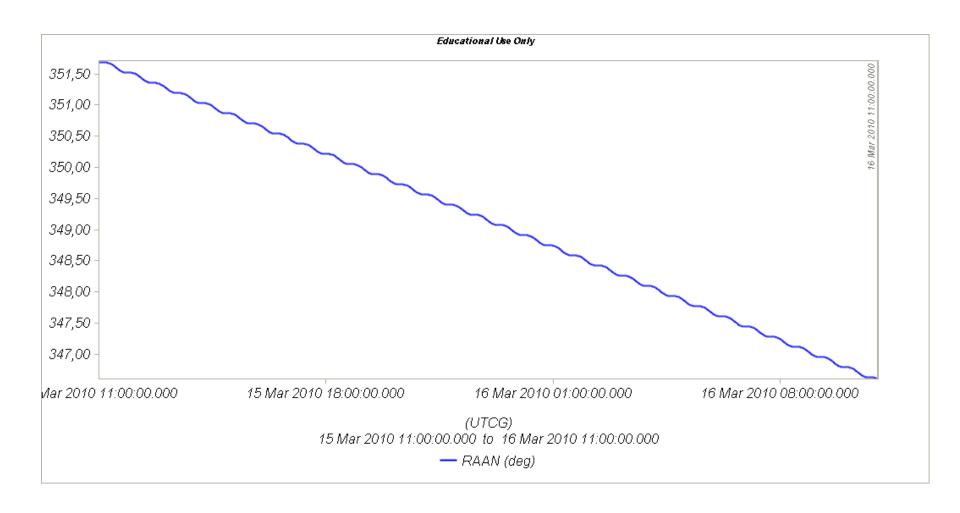
#### **STK: Analytic Propagator (SGP4)**

Several assumptions; propagation valid for short durations (3-10 days).

TLE data should be used as the input.

It considers secular and periodic variations due to Earth oblateness, solar and lunar gravitational effects, and orbital decay using a drag model.

#### **SGP4** Applied to ISS: RAAN



#### **Further Reading**

# SPACETRACK REPORT NO. 3

Models for Propagation of NORAD Element Sets

> Felix R. Hoots Ronald L. Roehrich

## **Secular Effects: Orders of Magnitude**

Orbit Class	Central Body			Drag	
Secular Effects	Ω	ω		. а	e
	°/day	°/day	-	m/day	/day
LEO	-5.7	6.5		5000	
Shuttle	5	5			
Mir	5.0	3.8			
Landsat	1	-3.1		100	
DMSP	1	-2.9			
TOPEX	-2.1	-0.5			
LAGEOS I	0.3	-0.2			
ICO	0.1	0.1			
GPS	~	~			
Molniya	-0.2			100	

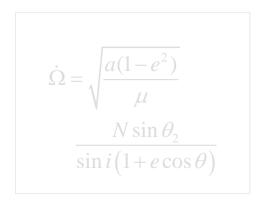
Vallado, Fundamental of Astrodynamics and Applications, Kluwer, 2001.

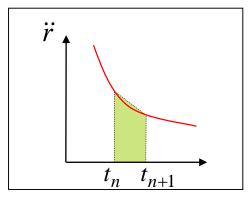
#### **Periodic Effects: Orders of Magnitude**

Orbit Class		Centra	ıl Body		Drag	Third Body	Solar Radiation
Periodic Effects	SP	m-daily	lin com	Res			
	m	m	m	m	m	m	m
LEO							
Shuttle	7000	470	50	Deep	33	0.5	~
Mir	6000	380	46		3	0.3	~
Landsat	9100	610	36		~		
DMSP	9000	590	134		~	~	~
TOPEX	7200	445	334		~	1	~
LAGEOS I	4800	115	18			0.1	~
ICO	2000	40	23			10	10
GPS	1700	17	18	Deep		100	12
Molniya	32,000	105	900	Deep	50	250	10
GEO	1600	~	16	Deep		716	50

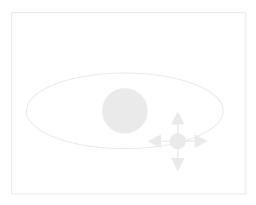
Vallado, Fundamental of Astrodynamics and Applications, Kluwer, 2001.

# 6. Non-Keplerian Motion





#### Numerical methods



#### **STK Propagators**

2-body: analytic propagator (constant orbital elements).

J2: analytic propagator (secular variations in the orbit elements due to Earth oblateness.

HPOP: **numerical integration** of the equations of motion (periodic and secular effects included).





Errors accumulation for long intervals

Computationally intensive

#### Real-Life Example: German Aerospace Agency

# ANALYSIS OF ORBIT PROPAGATION AND RELATIVE POSITION ACCURACY OF SMALL SATELLITES FOR SAR INTERFEROMETRY

Sergio De Florio, Dr. Thomas Neff, Tino Zehetbauer

DLR, Microwave and Radar Institute, Oberpfaffenhofen Münchner Straße 20, 82234 Weßling, Germany

Phone: +498153282357, Fax: +498153281452, Sergio.DeFlorio@dlr.de

Earth gravity field model	70x70 gravity coefficients of the 200x200 GRACE-GGM02C gravity model
Third body gravitational perturbation	Sun and Moon using highly accurate planetary ephemeris DE200 generated by JPL
Atmospheric density model	Jacchia-Roberts implemented with a $F_{10.7}$ (10.7 cm solar flux index) prediction file
Numerical integration	Runge Kutta 8(9) algorithm

#### Real-Life Example: German Aerospace Agency

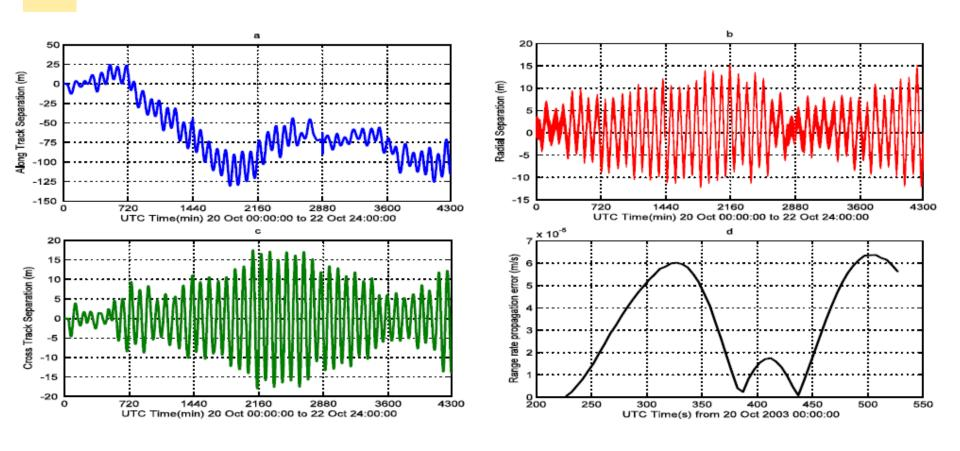


Figure 3. Propagation errors

propagation tool. The accuracy which can be reached with the presented method, after a propagation of  $\frac{3 \text{ days}}{3 \text{ days}}$ , is about  $\frac{10 - 15 \text{ m RMS}}{10 \text{ m RMS}}$  in cross-track and radial direction and about  $\frac{100 \text{ m RMS}}{100 \text{ m RMS}}$  in along-track direction.

#### **Further Reading on the Web Site**

# IMPACT OF ORBIT PREDICTION ACCURACY ON LOW EARTH REMOTE SENSING FLIGHT DYNAMICS OPERATIONS

Christian Arbinger<sup>(1)</sup>, Simone D'Amico<sup>(1)</sup>

(1) German Space Operations Center (DLR/GSOC), D-82234 Wessling (Germany), E-mail: christian.arbinger@dlr.de

This paper addresses the problem of orbit prediction and its impact on flight dynamics operations. In general, certain "knowledge" of the satellite's orbit is necessary to design and implement a ground-in-the-loop orbit control system. The operational constraints imposed by Low Earth Orbit (LEO) satellites and the stringent orbit control requirements driven by the use synthetic-aperture-radars (SAR) on board the satellites, give great importance to the orbit calculation chain.

#### **Real-Life Example: Envisat**

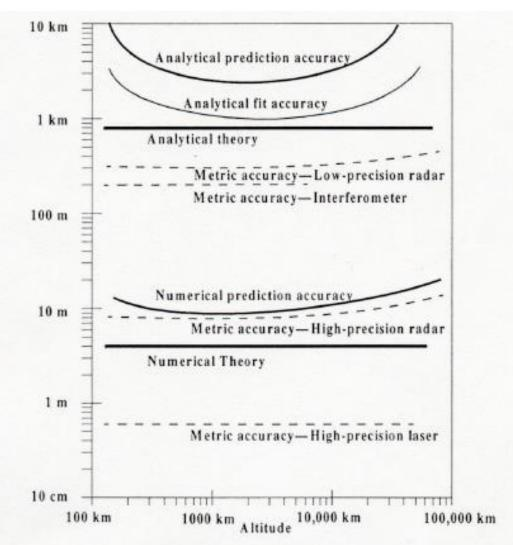
#### **Envisat Orbit Prediction Error**

The following table shows the RMS of the daily computed along-track errors over 1 orbit after 1, 3, and 6 days of Envisat orbit prediction.

#### Envisat (meters)

Month	after 1 day	after 3 days	after 6 days
December 2008	12	49	160
November 2008	12	54	194
October 2008	11	46	148
September 2008	11	38	128
August 2008	11	50	159
July 2008	12	47	144
June 2008	12	45	161
May 2008	14	47	127
May 2008	14	47	127
April 2008	12	51	173
March 2008	11	42	122

http://nng.esoc.esa.de/envisat/ ENVpred.html



Why do the predictions degrade for lower altitudes?

Errors in Determining a Satellite's Position. This figure (Knowles, 1995) shows general trends for typical accuracies of numerical and analytical theories (solid lines). Semianalytical theories range from nearly numerical to nearly analytical, depending on their force models. Observations (dashed lines) tend to degrade at higher altitudes. Notice how predictions and propagations degrade the theoretical accuracies, especially for analytical theories with significant drag and third-body effects.

#### Did you Know?

NASA began the first complex numerical integrations during the late 1960s and early 1970s.





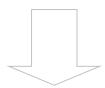
#### What is Numerical Integration?

$$\ddot{\mathbf{r}} = -\frac{\mu}{r^3}\mathbf{r} + \mathbf{a}_{perturbed}$$
 Given 
$$\mathbf{r}(t_n), \dot{\mathbf{r}}(t_n)$$
 
$$\Delta t = t_{n+1} - t_n$$

$$\mathbf{r}(t_{n+1}), \dot{\mathbf{r}}(t_{n+1})$$

#### **State-Space Formulation**

$$\ddot{\mathbf{r}} = -\frac{\mu}{r^3}\mathbf{r} + \mathbf{a}_{perturbed}$$



$$\dot{\mathbf{u}} = f(\mathbf{u}, t) \qquad \mathbf{u} = \begin{pmatrix} \mathbf{r} \\ \dot{\mathbf{r}} \end{pmatrix}$$

6-dimensional state vector

#### **How to Perform Numerical Integration?**

$$\mathbf{u}(t_n)$$



$$\mathbf{u}(t_{n+1})$$

$$f(t_n + h) = f(t_n) + hf'(t_n) + \frac{h^2}{2}f''(t_n) + \dots + \frac{h^s}{s!}f^{(s)}(t_n) + R_s$$

Taylor series expansion

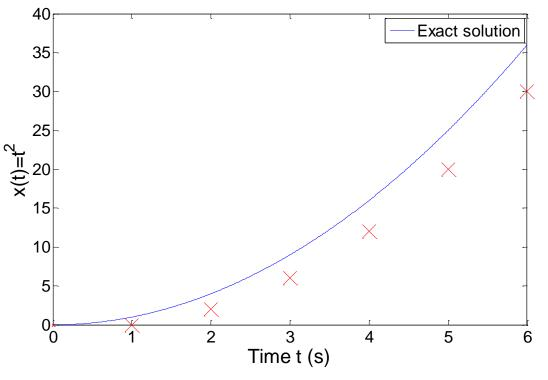
# First-Order Taylor Approximation (Euler)

#### along the tangent

$$\mathbf{u}(t_n + \Delta t) = \mathbf{u}(t_n) + \Delta t \, \dot{\mathbf{u}}(t_n)$$

$$\mathbf{u}_{n+1} = \mathbf{u}_n + \Delta t \, f(\mathbf{u}_n, t_n)$$

Euler step



The stepsize has to be extremely small for accurate predictions, and it is necessary to develop more effective algorithms.

#### **Numerical Integration Methods**

$$\mathbf{u}_{n+1} = \sum_{j=1}^{m} \alpha_{j} \mathbf{u}_{n+1-j} - \Delta t \sum_{j=0}^{m} \beta_{j} \dot{\mathbf{u}}_{n+1-j}$$

$$\rightarrow \text{State vector}$$

$$\beta_0 \neq 0$$

Implicit, the solution method becomes iterative in the nonlinear case

$$\beta_0 = 0$$

**Explicit**,  $\mathbf{u}_{n+1}$  can be deduced directly from the results at the previous time steps

$$\alpha_j$$
,  $\beta_j = 0$  for  $j > 1$ 

**Single-step**, the system at time  $t_{n+1}$  only depends on the previous state  $t_n$ 

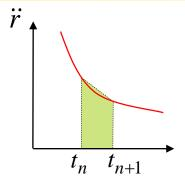
$$\alpha_j, \beta_j \neq 0$$
for  $j > 1$ 

**Multi-step**, the system at time  $t_{n+1}$  depends several previous states  $t_n, t_{n-1}$ , etc.

#### **Examples: Implicit vs. Explicit**

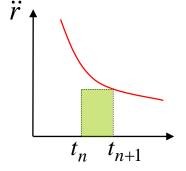
⇒ Trapezoidal rule (implicit)

$$\mathbf{u}_{n+1} = \mathbf{u}_n + \Delta t \, \frac{\left(\dot{\mathbf{u}}_n + \dot{\mathbf{u}}_{n+1}\right)}{2}$$



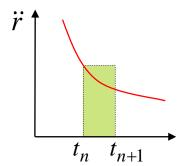
⇒ Euler backward (implicit)

$$\mathbf{u}_{n+1} = \mathbf{u}_n + \Delta t \ \dot{\mathbf{u}}_{n+1}$$



⇒ Euler forward (explicit)

$$\mathbf{u}_{n+1} = \mathbf{u}_n + \Delta t \ \dot{\mathbf{u}}_n$$



#### Why Different Methods?

A variety of methods has been applied in astrodynamics. Each of these methods has its own advantages and drawbacks:

Accuracy: what is the order of the integration scheme?

Efficiency: how many function calls?

Versatility: can it be applied to a wide range of problems?

Complexity: is it easy to implement and use?

Step size: automatic step size control?

#### Runge-Kutta Family: Single-Step

Perhaps the most well-known numerical integrator.

Difference with traditional Taylor series integrators: the RK family only requires the first derivative, but several evaluations are needed to move forward one step in time.

Different variants: explicit, embedded, etc.

# Runge-Kutta Family: Single-Step

$$\dot{\mathbf{u}}(t) = f(\mathbf{u}, t)$$
 with  $\mathbf{u}(t_0) = \mathbf{u}_0$ 

Slopes at various points within the integration step 
$$\mathbf{u}_{n+1} = \mathbf{u}_n + \Delta t \sum_{i=1}^{s} b_i \mathbf{k}_i$$

$$\mathbf{k}_1 = f\left(\mathbf{u}_n, t_n + c_1 \Delta t\right)$$

$$\mathbf{k}_i = f\left(\mathbf{u}_n + \Delta t \sum_{j=1}^{i-1} a_{ij} \mathbf{k}_j, t_n + c_i \Delta t\right), i = 2...s$$

#### Runge-Kutta Family: Single-Step

The Runge-Kutta methods are fully described by the coefficients:

Butcher Tableau

$$\mathbf{u}_{n+1} = \mathbf{u}_n + \Delta t \frac{\mathbf{k}_1 + 2\mathbf{k}_2 + 2\mathbf{k}_3 + \mathbf{k}_4}{6}$$

$$\mathbf{k}_1 = f\left(\mathbf{u}_n, t_n\right)$$

$$\mathbf{k}_2 = f\left(\mathbf{u}_n + \mathbf{k}_1 \frac{\Delta t}{2}, t_n + \frac{\Delta t}{2}\right)$$

$$\mathbf{k}_{3} = f\left(\mathbf{u}_{n} + \mathbf{k}_{2} \frac{\Delta t}{2}, t_{n} + \frac{\Delta t}{2}\right)$$

$$\mathbf{k}_4 = f\left(\mathbf{u}_n + \mathbf{k}_3 \Delta t, t_n + \Delta t\right)$$

Butcher Tableau

$$\mathbf{u}_{n+1} = \mathbf{u}_n + \Delta t \frac{\mathbf{k}_1 + 2\mathbf{k}_2 + 2\mathbf{k}_3 + \mathbf{k}_4}{6}$$

Estimated slope (weighted average)

$$\mathbf{k}_1 = f\left(\mathbf{u}_n, t_n\right)$$

Slope at the beginning

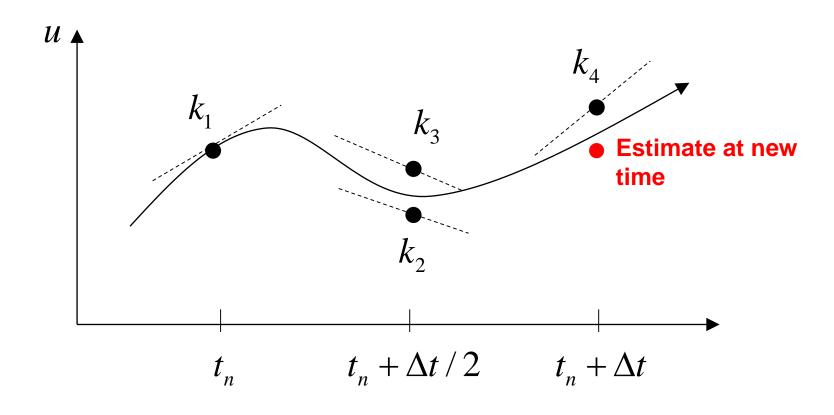
$$\mathbf{k}_2 = f\left(\mathbf{u}_n + \mathbf{k}_1 \frac{\Delta t}{2}, t_n + \frac{\Delta t}{2}\right)$$
 Slope at the midpoint (k<sub>1</sub> is used to determine the value of u – Euler)

of u – Euler)

$$\mathbf{k}_3 = f\left(\mathbf{u}_n + \mathbf{k}_2 \frac{\Delta t}{2}, t_n + \frac{\Delta t}{2}\right)$$
 Slope at the midpoint (k<sub>2</sub> is now used)

$$\mathbf{k}_4 = f\left(\mathbf{u}_n + \mathbf{k}_3 \Delta t, t_n + \Delta t\right)$$

Slope at the end



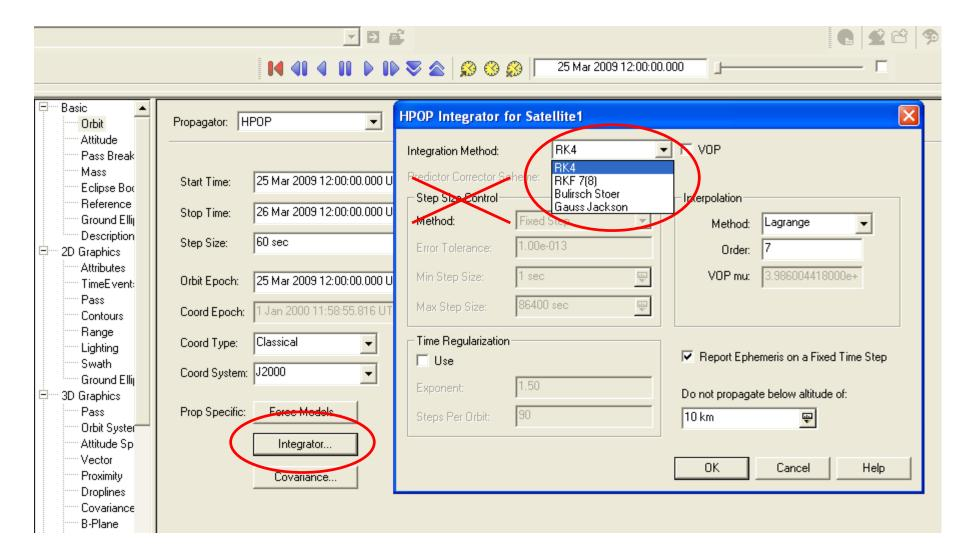
The local truncation error for a 4<sup>th</sup> order RK is  $O(h^5)$ .

The accuracy is comparable to that of a 4<sup>th</sup> order Taylor series, but the Runge-Kutta method avoids the calculation of higher-order derivatives.

Easy to use and implement.

The step size is fixed.

#### **RK4 in STK**



#### **Embedded Methods**

They produce an estimate of the local truncation error:

⇒ adjust the step size to keep local truncation errors within some tolerances.

This is done by having two methods in the tableau, one with order p and one with order p+1, with the same set of function evaluations:

$$\mathbf{u}_{n+1}^{(p)} = \mathbf{u}_n^{(p)} + \Delta t \sum_{i=1}^s b_i^{(p)} \mathbf{k}_i$$

$$\mathbf{u}_{n+1}^{(p+1)} = \mathbf{u}_n^{(p+1)} + \Delta t \sum_{i=1}^{s} b_i^{(p+1)} \mathbf{k}_i$$

#### **Embedded Methods**

The two different approximations for the solution at each step are compared:

If the two answers are in close agreement, the approximation is accepted.

If the two answers do not agree to a specified accuracy, the step size is reduced.

If the answers agree to more significant digits than required, the step size is increased.

#### Ode45 in Matlab / Simulink

Runge-Kutta (4,5) pair of Dormand and Prince:

- $\Rightarrow$  Variable step size.
- ⇒ Matlab help: *This should be the first solver you try*

0							
1/5	1/5						
3/10	3/40	9/40					
4/5	44/45	-56/15	32/9				
8/9	19372/6561	-25360/2187	64448/6561	-212/729			
1	9017/3168	-355/33	46732/5247	49/176	-5103/18656		
1	35/384	0	500/1113	125/192	-2187/6784	11/84	
	5179/57600	0	7571/16695	393/640	-92097/339200	187/2100	1/40
	35/384	0	500/1113	125/192	-2187/6784	11/84	0

#### Ode45 in Matlab / Simulink

```
Editor - C:\Program Files\MATLAB\R2007b\toolbox\matlab\funfun\ode45.m
File Edit Text Go Cell Tools Debug Desktop Window Help
                                           Stack: Base V
    * 4
                                      % % \ 1
              - 1.0
                          ÷ 1.1
258 -
           end
259 -
           nout = 1;
260 -
           tout(nout) = t;
                                                                              edit ode45
261 -
           yout(:,nout) = y;
262 -
         end
263
         % Initialize method parameters.
264
265 -
         pow = 1/5;
         A = [1/5, 3/10, 4/5, 8/9, 1, 1];
266 -
267 -
268
             1/5
                          3/40
                                  44/45
                                           19372/6561
                                                           9017/3168
                                                                            35/384
269
             0
                          9/40
                                  -56/15 -25360/2187
                                                           -355/33
270
             0
                          0
                                  32/9
                                           64448/6561
                                                           46732/5247
                                                                            500/1113
271
             0
                                  0
                                           -212/729
                                                           49/176
                                                                            125/192
272
             0
                          0
                                  0
                                           0
                                                           -5103/18656
                                                                            -2187/6784
273
             Π
                                                           0
                                                                            11/84
274
             0
                          Π
                                  0
                                           0
                                                                            0
275
             ];
         E = [71/57600; 0; -71/16695; 71/1920; -17253/339200; 22/525; -1/40];
276 -
277 -
         f = zeros(neq,7,dataType);
278 -
         hmin = 16*eps(t);
279 -
         if isempty(htry)
           % Compute an initial step size h using y'(t).
280
281 -
           absh = min(hmax, htspan);
```

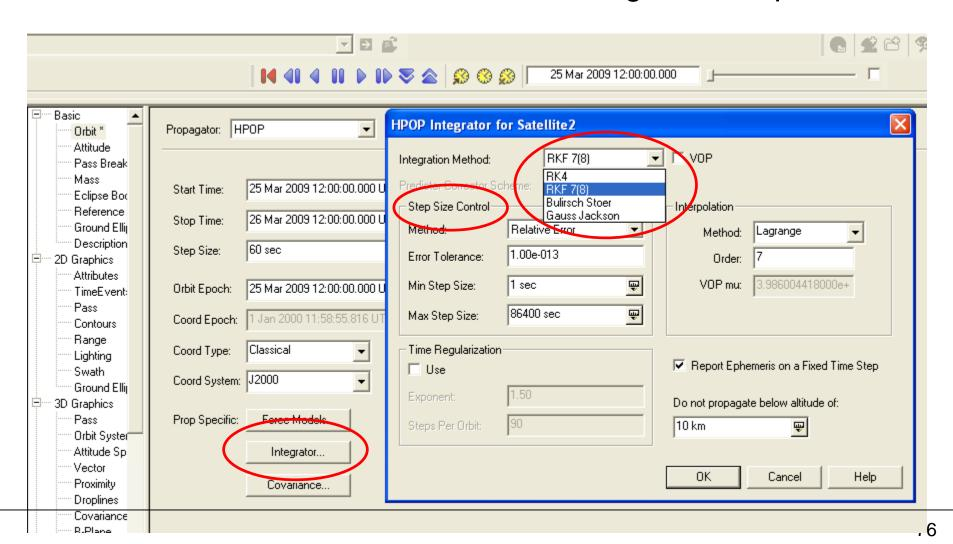
#### Ode45 in Matlab / Simulink

Be very careful with the default parameters!

options = odeset('RelTol',1e-8,'AbsTol',1e-8);

## RKF 7(8): Default Method in STK

Runge-Kutta-Fehlberg integration method of 7th order with 8th order error control for the integration step size.



0					Table	<b>5.3.</b> Fel	hlberg 7	7(8)					
$\begin{array}{c} 2 \\ \overline{27} \\ 1 \\ \overline{9} \\ 1 \\ \overline{6} \\ 5 \\ \overline{12} \\ 1 \\ \overline{2} \\ 5 \\ \overline{6} \\ \end{array}$	$   \begin{array}{r}     \frac{2}{27} \\     \frac{1}{36} \\     \frac{1}{24} \\     \frac{5}{12} \\     \frac{1}{20} \\     -\frac{25}{108} \\     31   \end{array} $			$   \begin{array}{r}       \frac{25}{16} \\       \frac{1}{4} \\       \underline{125} \\       \hline       108   \end{array} $	$\frac{1}{5}$ $-\frac{65}{27}$ $61$	125 54 2	13						
$\frac{1}{6}$ $\frac{2}{3}$ $\frac{1}{3}$	300 2	0	0	$-\frac{53}{6}$	704 45	$-\frac{2}{9}$ $-\frac{107}{9}$	900 67 90	3					
$\frac{1}{3}$	$-\frac{91}{108}$	0	0	$\frac{23}{108}$	$-\frac{976}{135}$	$\frac{311}{54}$	$-\frac{19}{60}$	$\frac{17}{6}$	$-\frac{1}{12}$				
1,	$\frac{2383}{4100}$	0	0	$-\frac{341}{164}$	$\frac{4496}{1025}$	$-\frac{301}{82}$	$\frac{2133}{4100}$	$\frac{45}{82}$	$\frac{45}{164}$	$\frac{18}{41}$			
0	$\frac{3}{205}$	0	0	0	0	$-\frac{6}{41}$	$-\frac{3}{205}$	$-\frac{3}{41}$	$\frac{3}{41}$	$\frac{6}{41}$	0		
1	$-\frac{1777}{4100}$	0	0	$-\frac{341}{164}$	$\frac{4496}{1025}$	$-\frac{289}{82}$	$\frac{2193}{4100}$	$\frac{51}{82}$	$\frac{33}{164}$	$\frac{12}{41}$	0	1	
$y_1$	41 840	0	0	0	0	$\frac{34}{105}$	$\frac{9}{35}$	$\frac{9}{35}$	9 280	$\frac{9}{280}$	$\frac{41}{840}$	0	0
$\widehat{y}_1$	0	0	0	0	0	$\frac{34}{105}$	9 35	9 35	$\frac{9}{280}$	$\frac{9}{280}$	0	$\frac{41}{840}$	$\frac{41}{840}$

## **Integrator Selection**

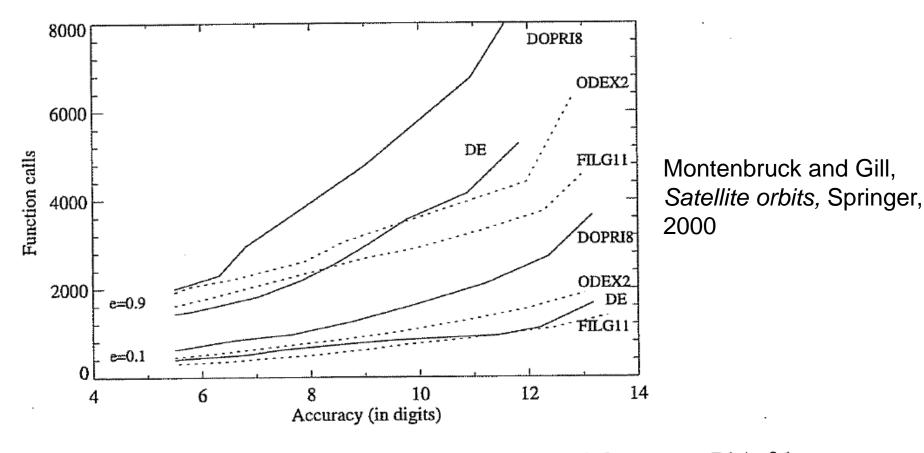


Fig. 4.9. Performance diagram of several single- and multistep methods for test cases D1 (e=0.1, lower set of curves) and D5 (e=0.9, upper set of curves) of Hull et al. (1972). The number of function calls is plotted versus the relative accuracy in digits.

# Why is the Step Size So Critical?

### Theoretical arguments:

- 1. The accuracy and the stability of the algorithm are directly related to the step size.
- 2. Nonlinear equations of motion.

Data for Landsat 4 and 6 in circular orbits around 800km indicates that a one-minute step size yields about 47m error.

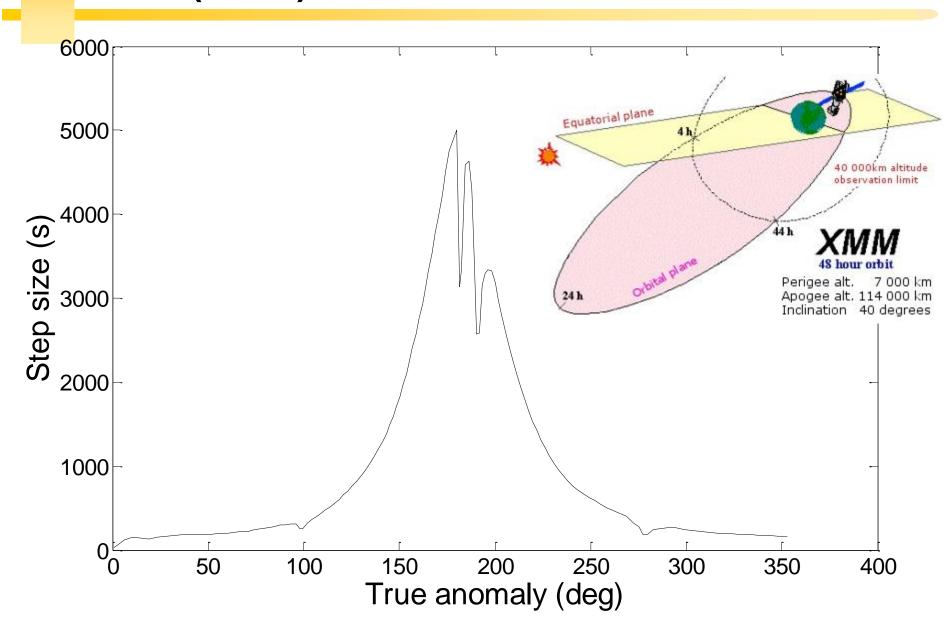
A three-minute step size produces about a 900m error!

# Why is the Step Size So Critical?

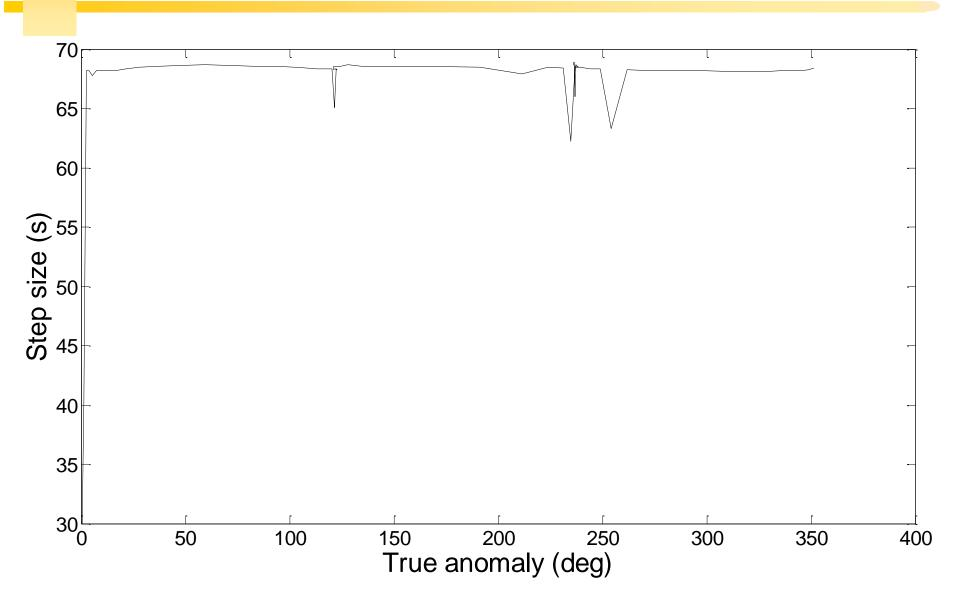
### More practical arguments:

- 1. The computation time is directly related to the step size.
- 2. The particular choice of step size depends on the most rapidly varying component in the disturbing functions (e.g., 50 x 50 gravity field).

# XMM (e~0.8)



# ISS(e~0)



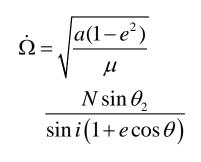
#### "Difficult" Orbits

Automatic time step is especially nice on highly eccentric orbits (Molniya, XMM). These orbits are best computed using variable step sizes to maintain some given level of accuracy:

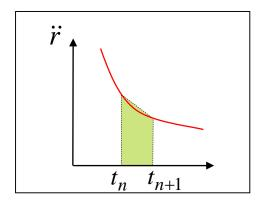
Without this variable step size, we waste a lot of time near apoapsis, when the integration is taking too small a step.

Likewise, the integrator may not be using a small enough step size at periapsis, where the satellite is traveling fast.

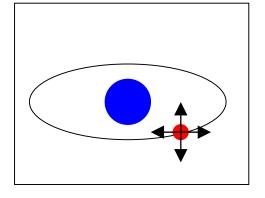
# 6. Non-Keplerian Motion



Analytic treatment



Numerical methods



ISS and geostationary satellites

# **ISS Example**

1. Earth's oblateness only

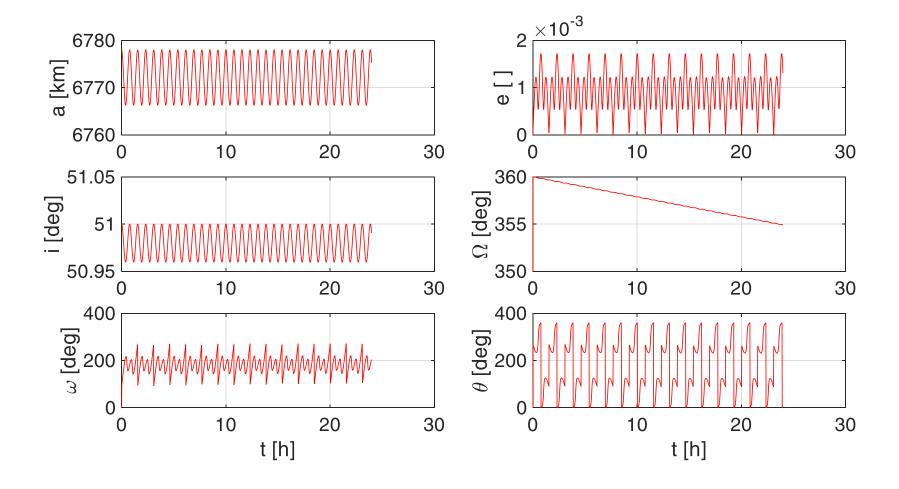
2. Drag only

3. Sun and moon only

4. SRP only

5. All together.

# J2 Only



### Overall Effects of the J2 Perturbation

Nodal regression: regression of the nodal line:

$$\dot{\Omega}_{avg} = \frac{1}{T} \int_0^T \dot{\Omega} \, dt = - \left[ \frac{3}{2} \frac{\sqrt{\mu} J_2 R^2}{(1 - e^2)^2 a^{7/2}} \right] \cos i$$

Apsidal rotation: rotation of the apse line:

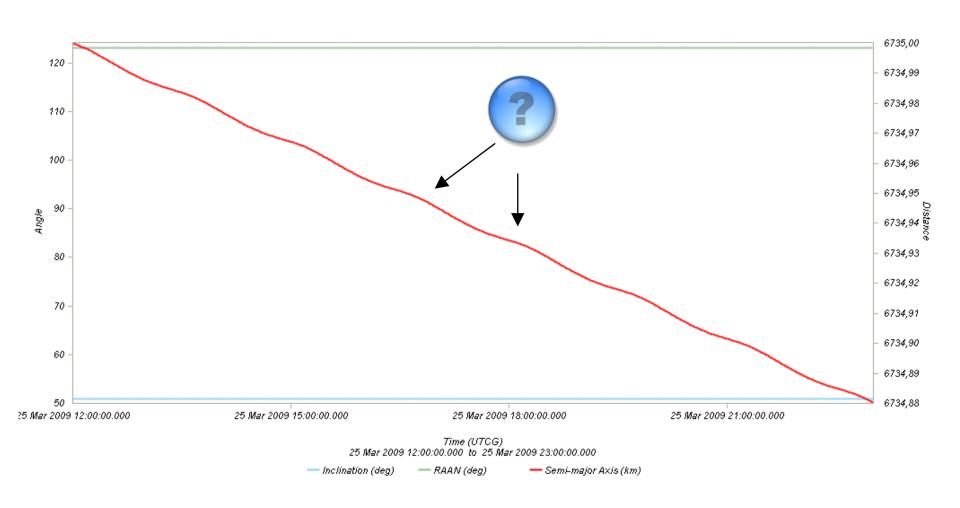
$$\dot{\omega}_{avg} = \frac{1}{T} \int_0^T \dot{\omega} \, dt = \left[ \frac{3}{4} \frac{\sqrt{\mu} J_2 R^2}{(1 - e^2)^2 a^{7/2}} \right] (4 - 5\sin^2 i)$$

Mean anomaly.

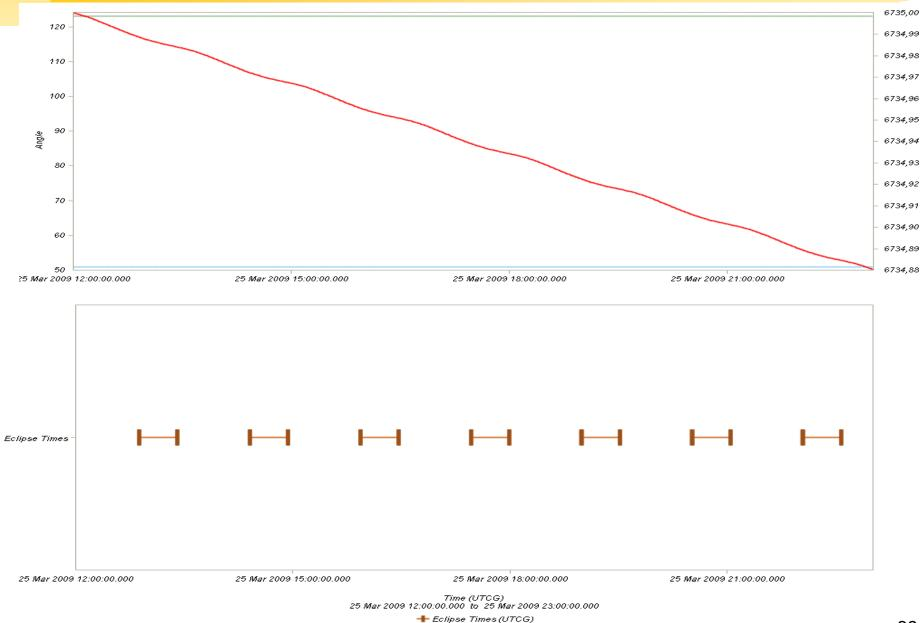
No secular variations for *a*, *e*, *i* because we have a conservative perturbation.

## Drag Only: i, $\Omega$ , a

# HPOP with drag – Harris Priester (without oblateness/SRP/Sun and Moon)

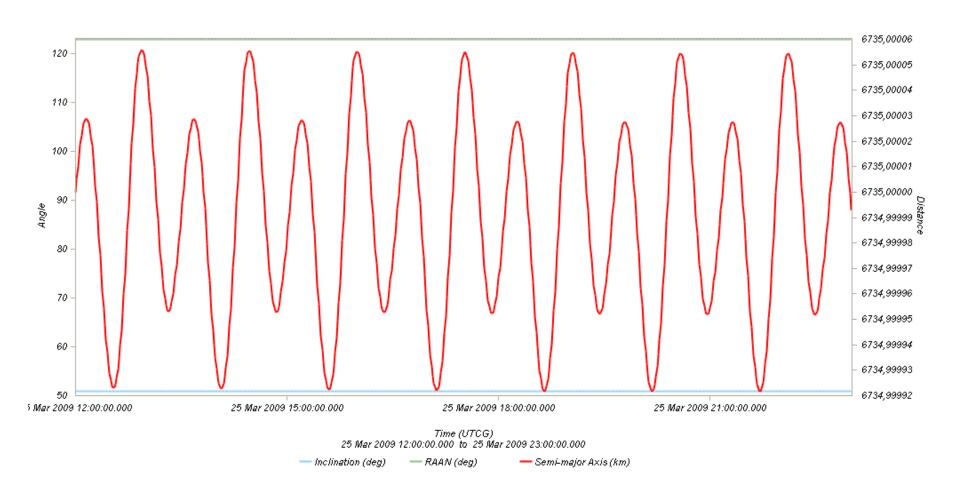


# **Drag: Relationship with Eclipses**

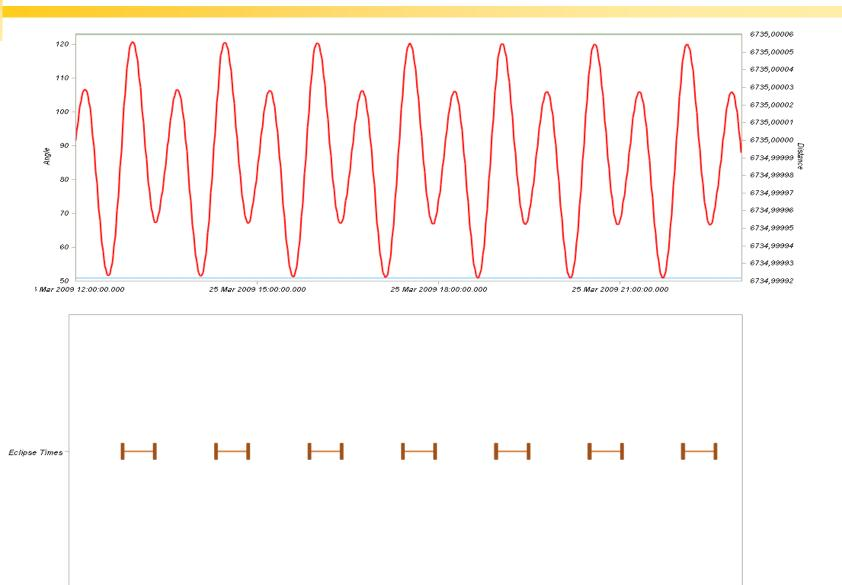


## SRP Only: i, $\Omega$ , a

# HPOP with SRP (without oblateness/drag/Sun and Moon)



# **SRP: Relationship with Eclipses**



Time (UTCG)
25 Mar 2009 12:00:00.000 to 25 Mar 2009 23:00:00.000
+ Eclipse Times (UTCG)

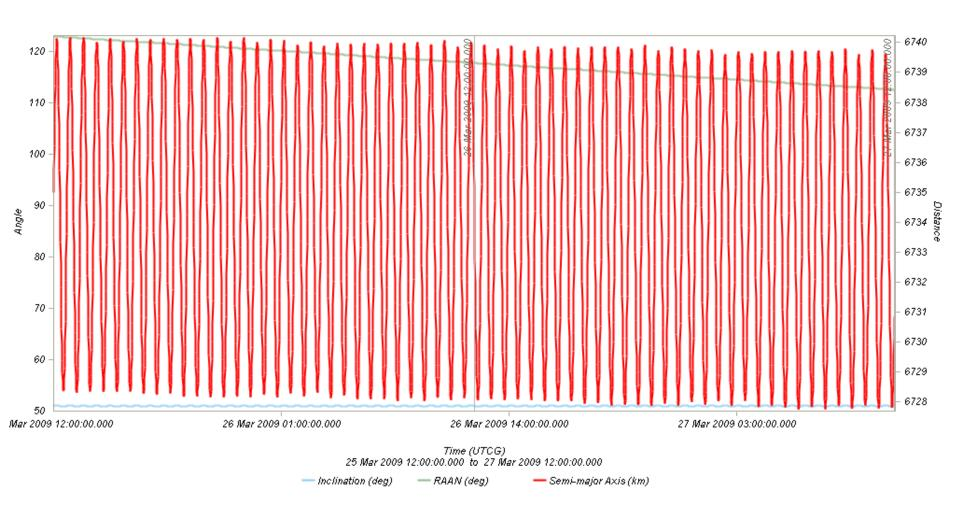
25 Mar 2009 15:00:00.000

25 Mar 2009 18:00:00.000

25 Mar 2009 21:00:00.000

25 Mar 2009 12:00:00.000

# **All Perturbations Together**



#### **GEO Satellites**

#### Nice illustration of:

- 1. Perturbations of the 2-body problem.
- 2. Secular and periodic contributions.
- 3. Accuracy required by practical applications.
- 4. The need for orbit correction and thrust forces.

And it is a real-life example (telecommunications, meteorology)!

## **Three Main Perturbations for GEO Satellites**

1. Non-spherical Earth

2. SRP

3. Sun and Moon

# **Station Keeping of GEO Satellites**

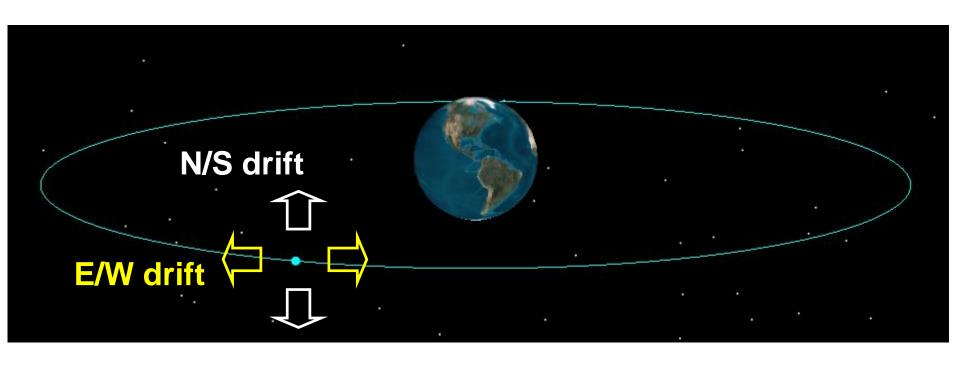
The effect of the perturbations is to cause the spacecraft to drift away from its nominal station. If the drift was allowed to build up unchecked, the spacecraft could become useless.

A station-keeping box is defined by a longitude and a maximum authorized distance for satellite excursions in longitude and latitude.

For instance, TC2:  $-8^{\circ} \pm 0.07^{\circ}$  E/W  $\pm 0.05^{\circ}$  N/S

### **East-West and North-South Drift**

What are the perturbations generating these drifts?



### **East-West Drift**

A GEO satellite drifts in longitude due to the influence of two main perturbations:

 The elliptic nature of the Earth's equatorial crosssection: J22 (and not from the N/S oblateness J2).

2.  $\bigvee_{\text{sat}} \bigvee_{\text{v}} \bigvee_{\text{sat}} \bigvee_{\text{v}} \bigvee_{\text{sat}} \bigvee_{\text{v}} \bigvee_{\text{sat}} \bigvee_{\text{v}} \bigvee_{v} \bigvee_{\text{v}} \bigvee_{$ 

## **East-West Drift due to Equatorial Ellipticity**

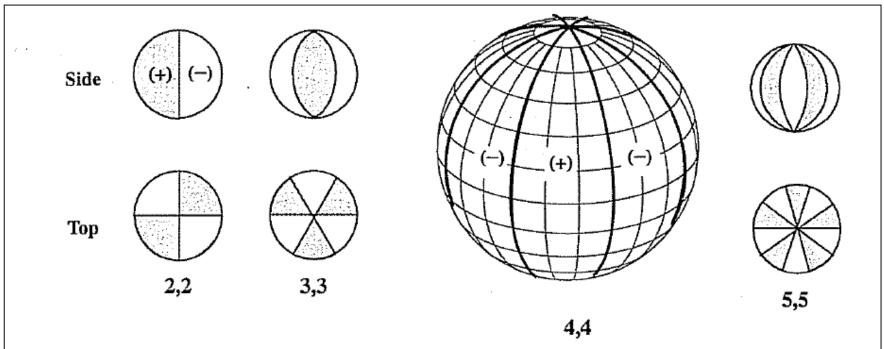


Figure 8-5. Sectorial Harmonics. Sectorial harmonics take into account the extra mass distribution in longitudinal regions.

## **East-West Drift due to Equatorial Ellipticity**

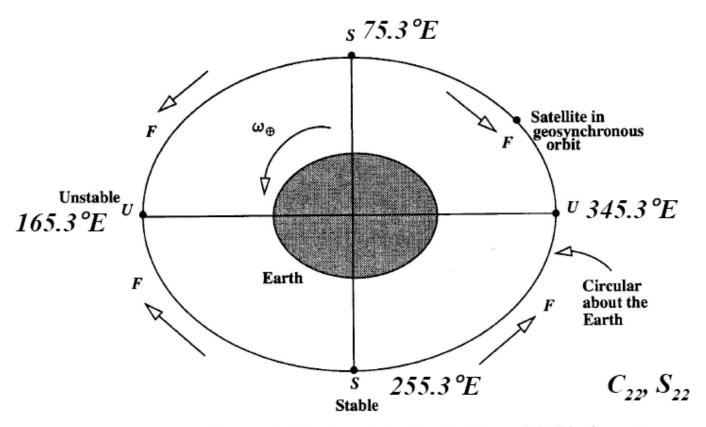
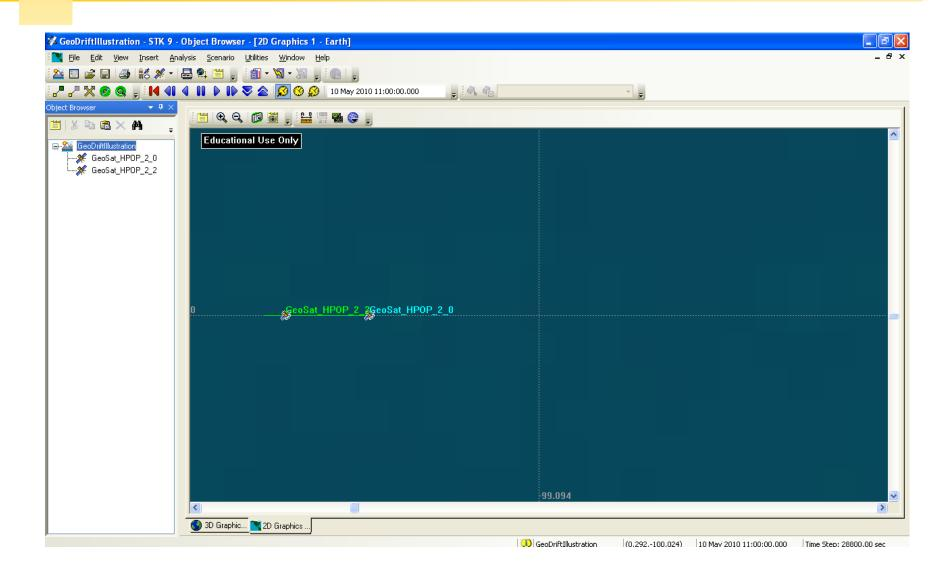


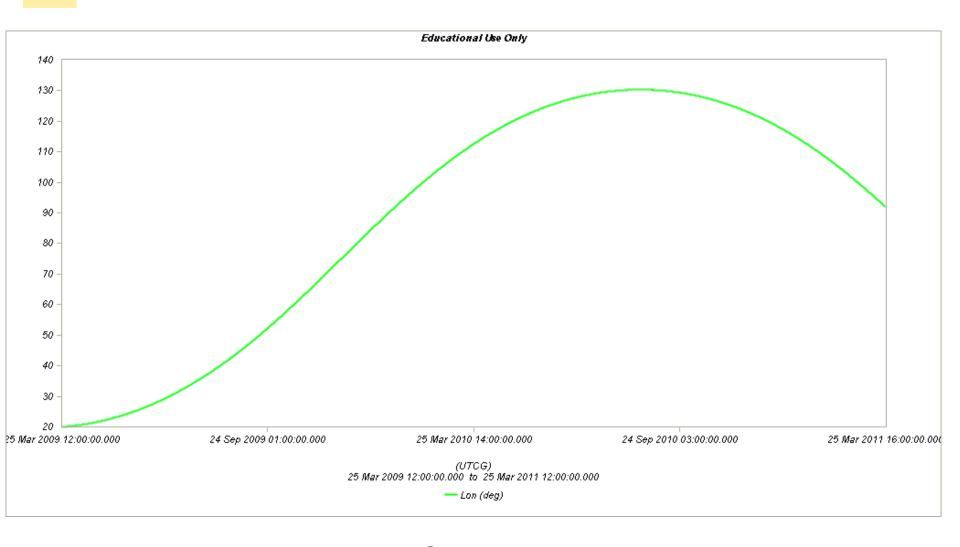
Figure 8-8. Polar View of an Equatorial Section of the Earth.  $(C_{22} \text{ only})$  F is the net tangential force on the satellite at the positions shown.  $C_{22}$  models a longitudinal asymmetry of the Earth. Both stable (S) and unstable (U) positions are identified.

(Vallado, 1997)

## East-West Drift: HPOP (2,0) vs. HPOP (2,2)

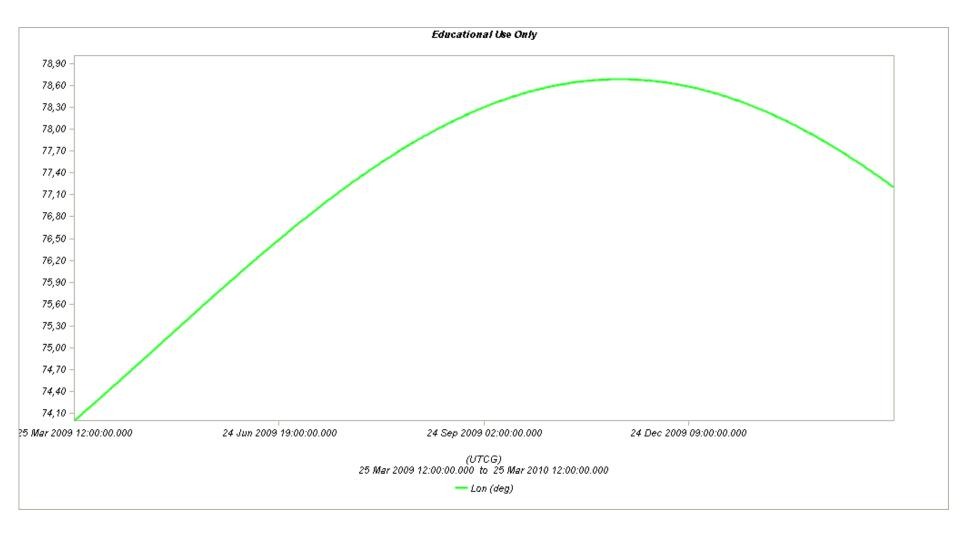


# **East-West Drift: Stable Equilibirum**



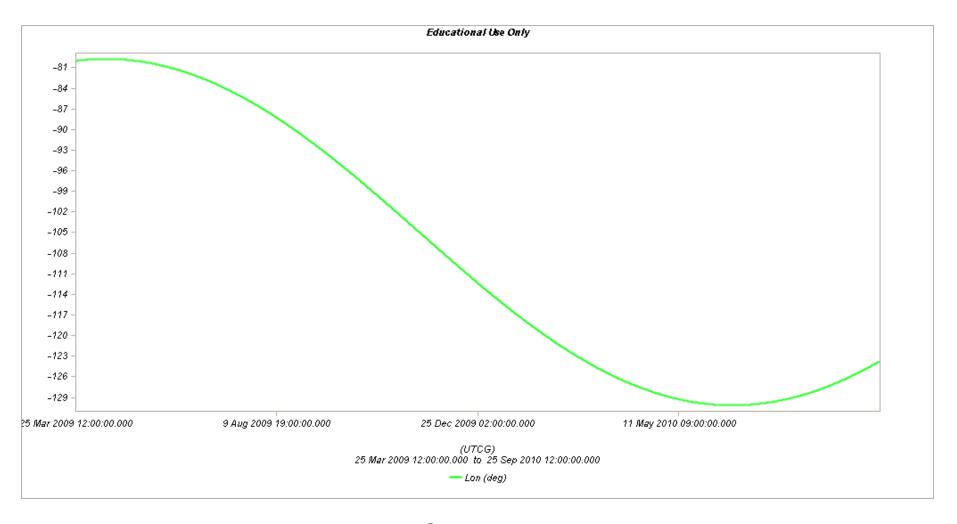
HPOP with 2,2 (without Sun and moon/SRP/drag)

## **East-West Drift: Stable Equilibirum**



HPOP with 2,2 (without Sun and moon/SRP/drag)

## **East-West Drift: Stable Equilibirum**



HPOP with 2,2 (without Sun and moon/SRP/drag)

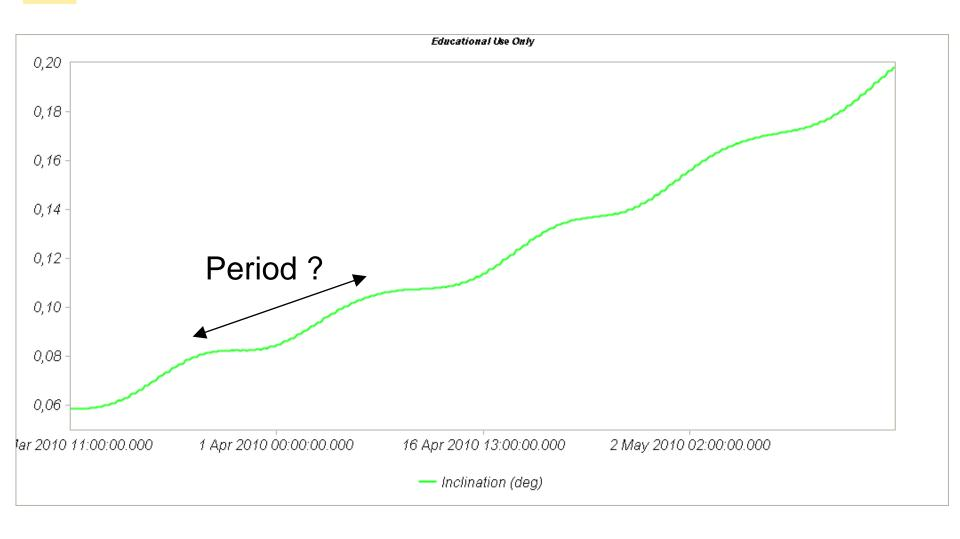
#### **North-South Drift**

The perturbations caused by the Sun and the Moon are predominantly out-of-plane effects causing a change in the inclination and in the right ascension of the orbit ascending node.

Similar effects on the orbit to those of the Earth's oblateness (but here with respect to the ecliptic)

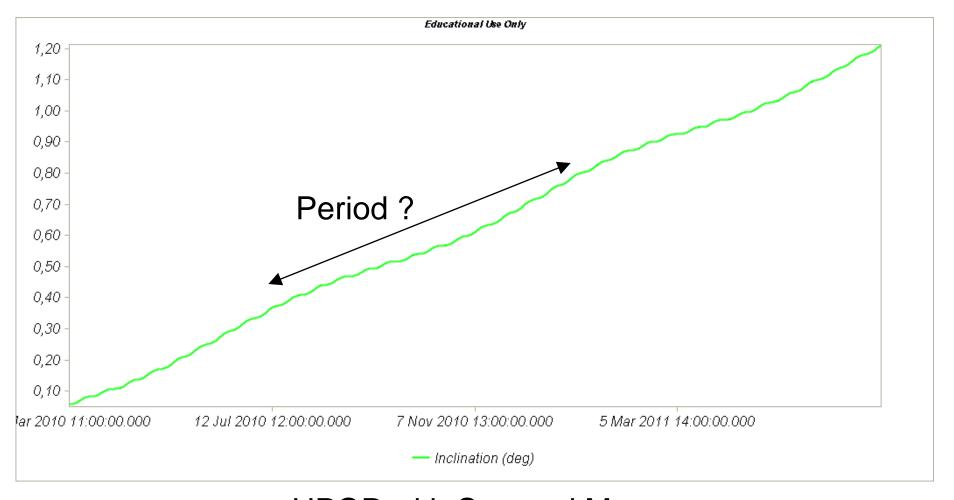
A GEO satellite therefore drifts in latitude with a fundamental period equal to the orbit period.

#### **North-South Drift**



HPOP with Sun and Moon (without oblateness/SRP/drag)

#### **North-South Drift**



HPOP with Sun and Moon (without oblateness/SRP/drag)

## **Thrust Forces for Stationkeeping**

GEO spacecraft require continual stationkeeping to stay within the authorized box using onboard thrusters.

Mission orbit Launcher Launch in GTO	Geostationary Proton	(Allowable dev	riation from nominal po	osition 0,1 deg	g)				
Mission duration (yrs) Maneuvre	15 delta v/maneuvre (m/s)	cycle time (days)	no. of maneuvers (-)	delta v/уг (m/s)	total delta V (m/s)				
Apogee kick	1836,49	*	1,0	*	1836,5				
10 yr average NSSK	10,73	86,1	63,6	45,5	682,0				
Worst Case NSSK	10,90	77,4	70,7	51,4	770,7				
EWSK	0,13	35,3	155,3	1,33	19,9				
Worst Case EWSK	NA	NA	NA	1,74	26,1				
Orbit Maneuvres	0,00	*	0,0	*	0,0				
Disposal	10,88	*	1,0	*	10,9				
		2549,3							
		2555,5							
		Total Delta V (worst case NSSK & EWSK)							

